Biomaterials 33 (2012) 2600–2607

Contents lists available at SciVerse ScienceDirect

Biomaterials

journal homepage: www.elsevier.com/locate/biomaterials

In vivo detection of glutathione disulfide and oxidative stress monitoring using a biosensor

Hui-Bog Noh [a], Pranjal Chandra [a], Jeon Ok Moon [b], Yoon-Bo Shim [a,*]

[a] Department of Chemistry and Institute of BioPhysio Sensor Technology, Pusan National University, Busan 609-735, Republic of Korea
[b] College of Pharmacy, Pusan National University, Busan 609-735, Republic of Korea

ARTICLE INFO

Article history:
Received 30 November 2011
Accepted 13 December 2011
Available online 30 December 2011

Keywords:
In vivo biosensor
Oxidative stress
Glutathione disulfide
β-nicotinamide adenine dinucleotide phosphate
Glutathione reductase
Conducting polymer

ABSTRACT

A highly sensitive in vivo biosensor for glutathione disulfide (GSSG) is developed using covalently immobilized-glutathione reductase (GR) and -β-nicotinamide adenine dinucleotide phosphate (NADPH) on gold nanoparticles deposited on poly[2,2′:5′,2″-terthiophene-3′-(*p*-benzoic acid)] (polyTTBA). The fabricated biosensor was characterized with SEM, TEM, XPS, and QCM. Analytical parameters affecting the biosensor performance were optimized in terms of applied potential, NADPH:GR ratio, temperature, and pH. A linear calibration plot is obtained using chronoamperometry in the dynamic range between 0.1 μM and 2.5 mM of GSSG, with a detection limit of 12.5 ± 0.5 nM. The developed biosensor is applied to detect GSSG in a real plasma sample. A microbiosensor was applied to detect the in vivo GSSG concentration to monitor the oxidative stress caused by diquat and *t*-butyl hydroperoxide. The results obtained are reliable, implying a promising approach for a GSSG biosensor in clinical diagnostics and oxidative stress monitoring.

1. Introduction

Glutathione, an important thiol tripeptide antioxidant (γ-glutamylcysteinylglycine) in cells, exists in two forms: one is a reduced form (GSH) and other is in oxidized form as glutathione disulfide (GSSG) [1]. In healthy living cells, more than 90% of glutathione is found as GSH, and less than 10% exists as GSSG. However, pathological conditions causing oxidative stress result in the conversion of GSH to its oxidized form, GSSG [2]. The high concentration of GSSG under oxidative stress conditions is associated with asthma [3], human immunodeficiency virus type 1 infection [4], and chronic renal failure [5]. Therefore, the analysis of the GSSG concentration in the body is important because it provides a sensitive index of whole body oxidative stress, as well as being helpful in the diagnosis of certain clinical disorder.

Various methods have previously been used to detect GSSG, which include the microplate reader assay [6], fluorimetry [7], and high-performance liquid chromatography (HPLC) [8–10]. However, these techniques all require an additional, time-consuming derivatization step. Electrochemical methods have also been used due to their simplicity, rapidity, high sensitivity, and low cost. These include the reduction of GSSG on a hanging mercury drop electrode [11], carbon nanotube modified electrode [10], and a nanoscale copper hydroxide composite carbon ionic liquid electrode [12]. The other advantage of electrochemical methods is that they can be miniaturized for in vivo measurements [13]. Microbiosensors for in vivo measurements offer several advantages such as rapid response time of a few sec, small feature sizes, capable of running a small sample volume, etc [13]. In recent years, considerable progress has been made in the application of enzyme-based microbiosensors to neurophysiology measurements such as dopamine, ATP and adenosine [14]. Though these microbiosensors provide a unique way to explore the microenvironments, there are limitations to be considered when designing them. Thus, we applied a newly synthesized monomer precursor of conducting polymer that result in the fabrication of stable, sensitive, and selective microbiosensor. The microbiosensor was examined to detect in vivo GSSG. It is important because it provides an index of whole body oxidative stress; however, no such study has been performed to date. Thus, it is necessary to develop a highly sensitive, stable, and simple detection method that can be used in biological fluids as well as for in vivo detection of GSSG.

It has been reported that GSSG is reduced to GSH in the presence of β-nicotinamide adenine dinucleotide phosphate (NADPH) and glutathione reductase (GR) [15]. Thus, NADPH and GR can be used as materials to fabricate a biosensor for GSSG detection. Conducting polymers are widely used in the fabrication of biosensors because

* Corresponding author. Tel.: +82 51 510 2244; fax: +82 51 514 2430.
E-mail address: ybshim@pusan.ac.kr (Y.-B. Shim).

0142-9612/$ – see front matter © 2011 Elsevier Ltd. All rights reserved.
doi:10.1016/j.biomaterials.2011.12.026

biomolecules can be covalently immobilized onto the conjugated polymer layers as they contain functional groups such as −COOH or $-NH_2$ [16–18]. The polymers, though biocompatible, are limited in use as base substrates for biosensors due to their low conductivity. Hence, gold nanoparticles (AuNPs) can be used for modifying the polymer layers to enhance the sensitivity of the biosensor [19,20]. Thus, our goal was to fabricate a GSSG biosensor through simultaneous immobilization of GR and NADPH onto the nanocomposite conducting polymer film.

In the present study, the biosensor probe was fabricated by immobilizing GR and NADPH through covalent bonding on a carboxylic acid group-functionalized conducting polymer (poly2,2′:5′,2″-terthiophene-3′-(*p*-benzoic acid), polyTTBA) layer on the AuNPs deposited glassy carbon electrode (GCE). The immobilization of GR and NADPH on the conducting polymer layer was confirmed using X-ray photon spectroscopy (XPS), a quartz crystal microbalance (QCM), cyclic voltammetry (CV), and linear sweep voltammetry (LSV). The fabricated biosensor was applied to detect GSSG with LSV and chronoamperometry. Various experimental parameters, such as applied potential, NADPH:GR ratio, temperature, and pH were optimized and the detection limit of GSSG was determined. The developed biosensor was successfully examined for spiked GSSG concentration in plasma samples. An in vivo microbiosensor was also fabricated by similar fabrication steps using a Pt microelectrode and successfully applied for GSSG detection in Sprague–Dawley rats treated with diquat and *t*-butyl hydroperoxide (*t*-BHP) to monitor oxidative stress, which was reflected by high concentrations of GSSG [21].

2. Experimental

2.1. Materials

A terthiophene monomer bearing a carboxylic acid group, (poly2,2′:5′,2″-terthiophene-3′-(*p*-benzoic acid), polyTTBA) was synthesized [19]. Tetrabutylammonium perchlorate (TBAP, electrochemical grade) was purchased from Fluka (USA) and purified according to a general method, followed by drying under vacuum at 1.33×10^{-3} Pa [22]. Glutathione disulfide (GSSG), β-nicotinamide adenine dinucleotide phosphate (NADPH), and glutathione reductase (GR, EC 1.6.4.2 from wheat germ, 0.043 U/mg solid) were purchased from Sigma Co. (USA). $HAuClO_4 \cdot 3H_2O$ and H_2SO_4 (99.999%) were purchased from Aldrich (USA). H_2O_2 was purchased from Sigma Co. (USA). 1-ethyl-3-(3-dimethylaminopropyl) carbodiimide (EDC), *N*-hydroxysuccinimide (NHS), diquat, *t*-butyl hydroperoxide (*t*-BHP), and dichloromethane (99.8%, anhydrous, sealed under N_2 gas) were purchased from Sigma Co. (USA). A phosphate buffer solution (PBS) was prepared using 0.1 M sodium dihydrogen phosphate and 0.1 M disodium hydrogen phosphate (Sigma–Aldrich). All aqueous solutions were prepared in ultra pure water, which was obtained from a Milli-Q water purifying system (18 MΩ cm).

2.2. Instruments

The cyclic voltammetric and amperometric experiments were performed with a potentiostat/galvanostat, Kosentech model KST P-2 (S. Korea). A three-electrode system was employed for voltammetry, where the modified GCE (dia. 3.0 mm) and platinum (Pt) microelectrode (dia. 100.0 μm), Ag/AgCl (saturated KCl), and a platinum wire were used as the working, reference, and auxiliary electrode, respectively. All of the electrodes were purchased from Kosentech Co. (S. Korea). The scanning electron microscope (SEM) images were obtained using a Cambridge Stereoscan 240. A JEOL JEM-2010 electron microscope (Jeol High-Tech. Co., Japan) with an acceleration voltage of 200 kV was used to obtain (transmission electron microscopy) TEM images. UV–visible spectra were obtained using UV-3101PC, Shimadzu (Japan). The QCM experiment was performed using a SEIKO EG & G model QCA 917 and a PAR model 263A potentiostat/galvanostat (USA). An Au-coated working electrode (area: 0.196 cm^2; 9.0 MHz; AT-cut quartz crystal) was used for the QCM experiment. The X-ray photospectroscopy (XPS) experiments were performed using a VG Scientific ESCALAB 250 XPS spectrometer with a monochromatic Al Kα source including charge compensation at KBSI (S. Korea).

2.3. Fabrication of GR-NADPH biosensor probe

To fabricate a biosensor, AuNPs were first electrodeposited onto the GCE in a 0.5 M H_2SO_4 solution containing 0.001% $HAuClO_4$ using linear sweep voltammetry (LSV) from +1.5 to +0.4 V. The electrodeposition conditions were as follows: 60.0 s deposition time, −0.60 V deposition potential, 100.0 mV/s scan rate, and the potential was cycled three times [20]. The polyTTBA layer was formed on the AuNPs/GCE through electropolymerization of 1.0 mM TTBA monomer in a 0.1 M TBAP/CH_2Cl_2 solution by a single potential cycle from 0.0 to +1.4 V at a scan rate of 100.0 mV/s [23]. For in vivo measurements, a microelectrode was manufactured according to procedures discussed in a previous work [13]. The final length of the Pt microelectrode was ~40 mm. The diameter of the microelectrode was 100.0 μm. The Pt microelectrode was cleaned by cycling the applied potential between +1.4 and −0.2 V for ten cycles at a scan rate of 200.0 mV/s in a 0.5 M H_2SO_4 solution, followed by washing with distilled water, where it was used in all subsequent experiments. The Pt microelectrode was modified with polyTTBA followed by GR and NADPH immobilization onto the polyTTBA coated microelectrode.

2.4. Electrochemical measurements

Cyclic voltammograms (CVs) were separately recorded for the polyTTBA/AuNPs/GC, NADPH/polyTTBA/AuNPs/GC, GR/polyTTBA/AuNPs/GC, and GR-NADPH/polyTTBA/AuNPs/GC electrodes from +0.25 to −0.35 V versus Ag/AgCl in 0.1 M PBS (pH 7.4). Chronoamperometric experiments were carried out using an applied potential of −0.70 V at the GR-NADPH/polyTTBA/AuNPs/GCE. Under the optimized conditions, GR-NADPH/polyTTBA/AuNPs/GCE was tested in different concentrations of GSSG. The chronoamperometric experiments were performed with consecutive injections into the measuring vessel in different concentrations of GSSG. All electrochemical experiments were performed in 0.1 M PBS with sodium sulfite (oxygen scavenger), and the solution was purged with nitrogen gas for 20.0 min to avoid any oxygen interference.

2.5. In vivo monitoring: animal studies

Adult male Sprague–Dawley rats (200.0–250.0 g) were obtained from Hyo-Chang Science Co. (Daegu, S. Korea). Rats were individually housed in a controlled environment during all experiments. Food and water were provided *ad libitum*, while maintaining a 6.0 h light/dark cycle. Animal handling was approved by the institutional animal care and use committee and was done in accordance with the provisions of the NIH "Guide for the Care and Use of Laboratory Animals". Appropriate amounts (200.0 μmol/kg) of diquat and *t*-BHP were separately administered intraperitoneally to monitor the oxidative stress. Controls experiments were performed by monitoring the GSSG level in rats that were not treated with diquat and *t*-BHP.

3. Results and discussion

3.1. Electrochemical behavior of GR-NADPH/polyTTBA/AuNPs/GCE

As shown in Scheme 1, electropolymerization of the TTBA monomer was performed on the AuNPs/GCE in dichloromethane. In the first anodic scan from 0.0 to +1.4 V, in a 1.0 mM TTBA monomer solution, the oxidation peak of the monomer appeared at +1.2 V, and in the reverse scan from +1.4 V, showed a small cathodic peak at +0.8 V, corresponding to a reduction of the oxidized polymer film formed in the first anodic scan (data not shown). These results are in agreement with those previously reported [23]. After polymerization, the carboxylic acid groups of the polyTTBA layer were activated with EDC/NHS, and GR and NADPH were simultaneously immobilized to form the GR-NADPH/polyTTBA/AuNPs/GCE biosensor. The formation of these modified electrodes was examined by CV.

Fig. 1 shows the CVs recorded for the (a) polyTTBA/AuNPs/GC, (b) NADPH/polyTTBA/AuNPs/GC, (c) GR/polyTTBA/AuNPs/GC, and (d) GR-NADPH/polyTTBA/AuNPs/GC electrodes in 0.1 M PBS (pH 7.4). No redox peaks were observed for the polyTTBA/AuNPs/GC. For the NADPH immobilized electrode, an oxidation peak at −0.05 V appeared due to the oxidation of NADPH. The oxidation peak position of NADPH was similar to previous reports [24]. In the case of the GR immobilized electrode, a redox peak at +0.087/+0.03 V (vs. Ag/AgCl) was observed due to the redox behavior of GR, which is consistent with previously reported results [25]. The results for the GR-NADPH electrode displayed two sets of redox peaks corresponding to GR and NADPH direct electrochemical processes, which clearly indicates the successful immobilization of GR and NADPH on the polyTTBA surface.

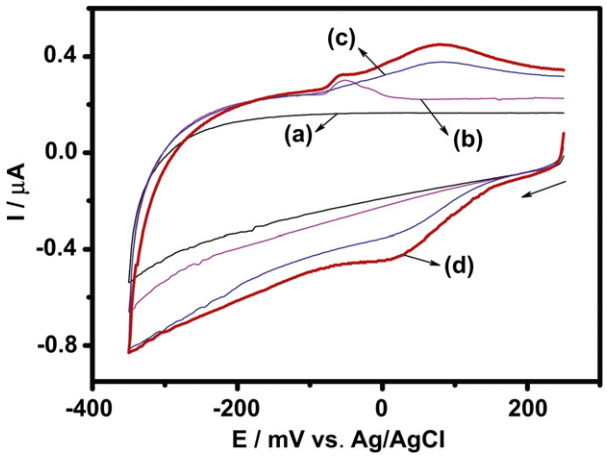

Fig. 1. CVs recorded for the (a) polyTTBA/AuNPs/GC (black line), (b) NADPH/polyTTBA/AuNPs/GC (magenta line), (c) GR/polyTTBA/AuNPs/GC (blue line), and (d) GR-NADPH/polyTTBA/AuNPs/GC (red line) electrodes in 0.1 M PBS (pH 7.4). (For interpretation of the references to colour in this figure legend, the reader is referred to the web version of this article.)

3.2. Characterization of the biosensor surface

In order to confirm the successful biosensor fabrication, the sensor probe was characterized using SEM, TEM, and XPS. Fig. 2(A) shows SEM images of the (a) AuNPs/GC, (b) polyTTBA/GC, and (c) polyTTBA/AuNPs/GC electrodes. The SEM image of the AuNPs/GC layer shows the presence of the AuNPs approximately 20.0 ± 1.5 nm in size (Fig. 2(A, a)). The morphology of the polyTTBA/AuNPs/GC layer shows a homogeneous layer of polyTTBA, while nanoparticles

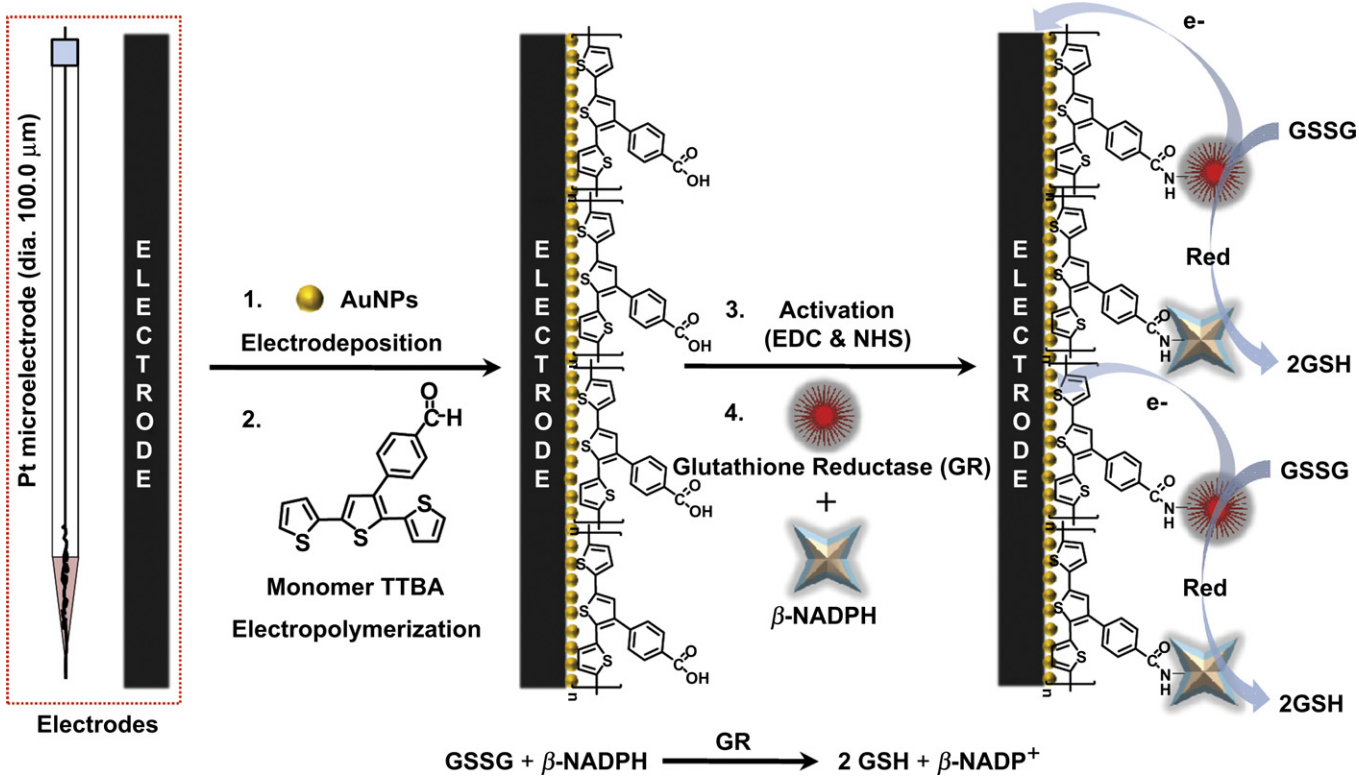

Scheme 1. Schematic preparation of the biosensors.

were not observed in this case due to the coverage of the electrode surface by the polyTTBA (Fig. 2(A, c)). An adsorption band at 522 nm in the UV–visible spectrum (data not shown) and the TEM image (Fig. 2(A, d)) confirmed that the particles size in this solution was ~20.0 nm. The modified electrodes were further characterized by XPS. All XPS spectra were taken after 50.0 s of Ar ion gas etching and calibrated using a C1s peak at 284.6 eV as an internal standard. Fig. 2(B) shows the XPS spectra of (a) Au4f, (b) S2p, (c) C1s, (d) N1s, and (e) O1s peaks for the polyTTBA/AuNPs/GC and GR-NADPH/polyTTBA/AuNPs/GC electrode surfaces. After electrodeposition of

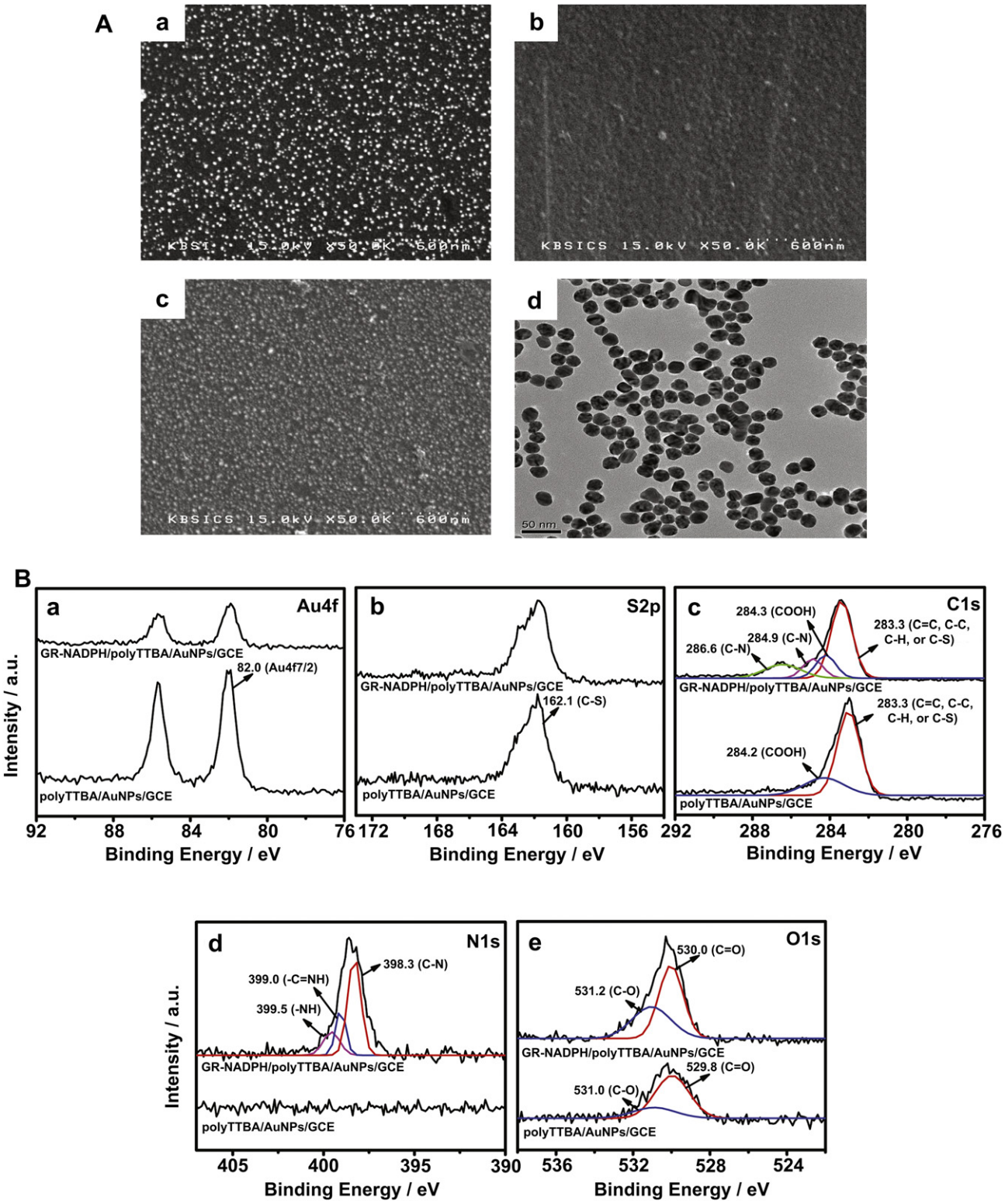

Fig. 2. (A) SEM images of (a) AuNPs/GC, (b) polyTTBA/GC, and (c) polyTTBA/AuNPs/GC electrodes and a TEM image of (d) AuNPs solution. (B) XPS spectra of the (a) Au4f, (b) S2p, (c) C1s, (d) N1s, and (e) O1s peaks for the polyTTBA/AuNPs/GC and GR-NADPH/polyTTBA/AuNPs/GC electrodes.

the AuNPs on the GC, two sharp peaks were observed at 82.0 and 85.6 eV (Fig. 2(B, a)). This implies the successful deposition of AuNPs onto the GC surface. The intensity of the peaks in the Au4f spectra of the polyTTBA/AuNPs electrode surface diminished after NADPH and GR were immobilized on the polymer film, indicating that the polyTTBA surface was covered with NADPH and GR (Fig. 2(B, a)). The S2p spectrum exhibited one peak at about 162.1 eV, corresponding to the C-S bonds for the polyTTBA layer. After immobilization of GR and NADPH, however, the intensity of this peak decreases, which also confirms the immobilization of GR and/or NADPH (Fig. 2(B, b)). The C1s spectrum of the polyTTBA exhibited two peaks at 283.0 and 284.2 eV, which correspond to the C═C, C-C, C-H, or C-S (red line) and COOH (blue line) bonds, respectively (Fig. 2(B, c)) [23]. Additional peaks were observed after the immobilization of GR and NADPH on the polyTTBA surface at 283.3 (C═C, C-C, C-H or C-S, red line), 284.3 (COOH, blue line), 284.9 (C-N, magenta line), and 286.6 eV (C═N, green line). The peaks at 283.0 and 284.2 eV are slightly shifted to higher binding energies, due to the formation of a covalent bond between the carboxylic acid groups in polyTTBA and the amine groups in GR and/or NADPH. The spectral deconvolution of N1s for the GR-NADPH/polyTTBA/AuNPs modified electrode shows clear peaks at 398.3 (red line), 399.0 (blue line), and 399.5 eV (magenta line) corresponding to C-N, -C═NH, and −NH bond formation, respectively, while no peak appeared in the case of the polyTTBA/AuNPs/GC (Fig. 2(B, d)). This indicates that NADPH and GR were successfully immobilized onto the polyTTBA layer. The O1s spectrum of polyTTBA exhibited two peaks at 529.8 (red line) and at 531.0 eV (blue line), which correspond to C═O and C-O, respectively. The peaks at C═O (530.0 eV, red line) and C-O (531.2 eV, blue line) are slightly shifted to higher energies after the immobilization of NADPH and GR (Fig. 2(B, e)).

Further studies were performed through QCM experiments to estimate the amount of GR and NADPH immobilized on the polymer film based on the frequency change (data not shown). In the case of NADPH immobilization, the decrease in frequency reaches a complete steady state after about 2.0 h, with an overall frequency change (Δf) of 0.14 kHz, corresponding to a mass change (Δm) of 152.8 ± 8.5 ng based on a previously defined equation [18]. The number of molecules per area for NADPH on the surface was determined to be 2.1×10^{-10} mol/cm^2. In the case of GR immobilization, the frequency decrease attained a steady state within 1.5 h, with an overall frequency change (Δf) of 0.40 kHz and a corresponding mass change (Δm) of 436.4 ± 12.5 ng. The number of molecules per area for GR on the surface was determined to be 4.4×10^{-12} mol/cm^2. These results confirm that GR and NADPH are successfully immobilized onto the polyTTBA layer.

3.3. Optimization of the analytical parameters

The analytical parameters for the detection of GSSG with the biosensor were optimized in terms of applied potential, NADPH:GR ratio, temperature, and pH, where the GSSG concentration was kept constant. First, the effect of the applied potential on the electrochemical reduction of GSSG was studied between −0.45 and −0.75 V (Fig. 3(a)). The reduction current gradually increased from −0.45 to −0.70 V but did not increase significantly over −0.70 V. Thus, −0.70 V was used in subsequent experiments. The effect of the relative amounts of GR and NADPH immobilized on biosensor performance was investigated for a range of

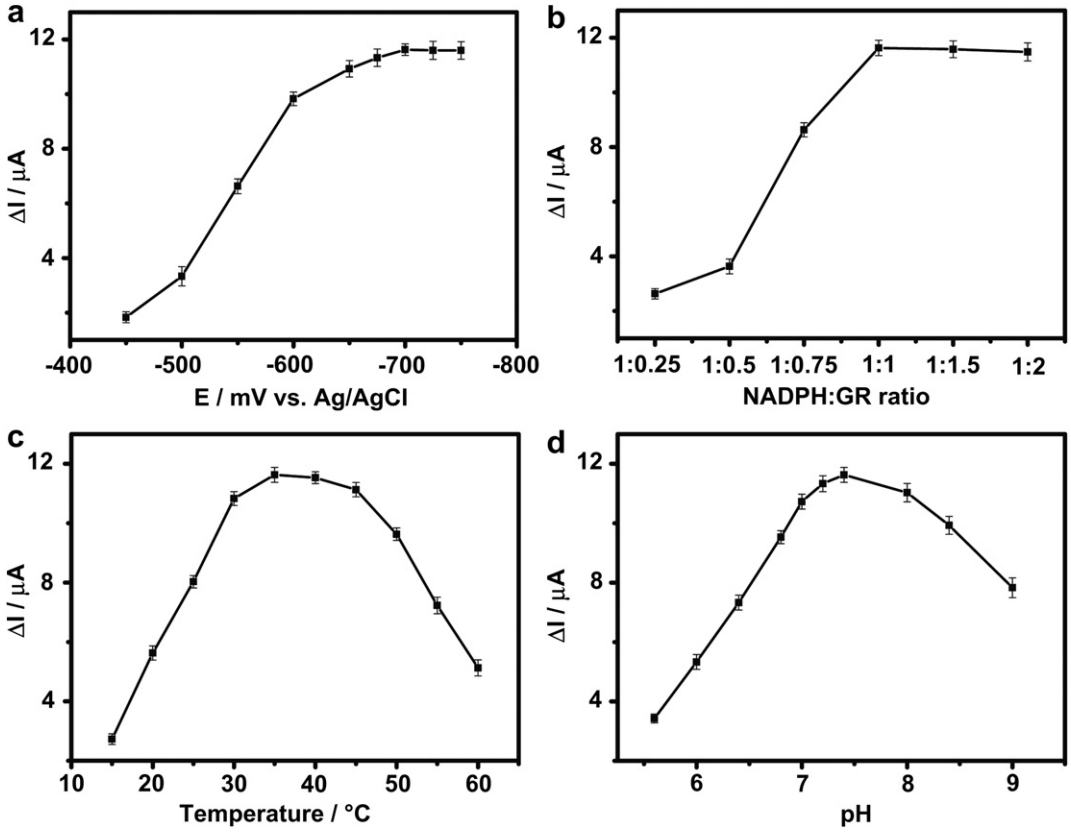

Fig. 3. Effects of the (a) applied potential, (b) NADPH:GR ratio, (c) temperature, and (d) pH on the LSV peak currents obtained for the GR-NADPH/polyTTBA/AuNPs/GCE in 0.5 mM GSSG.

NADPH:GR from 1.0:0.25 up to 1.0:2.0 (Fig. 3(b)). The current response gradually increased up to a ratio of NADPH:GR of 1:1 and then remained stable. Thus, this ratio of NADPH:GR was selected as the optimum ratio for analytical performance of the fabricated biosensor. The effect of temperature on the performance of the biosensor was studied between 15 and 60 °C (Fig. 3(c)). The current response increased as the temperature increased from 15 to 35 °C, and the current response decreased as with the temperature increased from 35 to 60 °C due the deactivation of GR-NADPH. The optimized temperature is almost similar to the body temperature employing use of fabricated biosensor in in vivo GSSG detection. On the basis of temperature dependency, 35 °C was selected for further experiments. The effect of pH on GSSG detection was studied over a range of 5.6–9.0. (Fig. 3(d)). The reduction current gradually increased as pH increased from pH 5.6 to 7.4 and decreased with a further increase in pH up to 9.0. The maximum reduction current was observed at a pH of 7.4. The maximum response of pH 7.4 was possibly due to the highest enzyme activity. In addition, in high acidic or alkaline pH, the GR is irreversibly inactivated [26]. The optimized pH was similar to the pH of extracellular fluids in the human body, making the proposed biosensor desirable for use in biological fluids. Thus, pH 7.4 was selected as the optimum pH for subsequent experiments.

3.4. Analytical performance of the GR-NADPH/polyTTBA/AuNPs/GCE

Analytical performance of the GR-NADPH/polyTTBA/AuNPs/GC biosensor was examined under the optimized conditions. The biosensor was dipped into 0.1 M PBS (blank/no GSSG), and the LSV was recorded by potential sweep between +0.25 and −0.75 V (vs. Ag/AgCl) (Fig. 4 (A)). A reduction peak at +0.03 V (vs. Ag/AgCl) was observed due to the reduction process of the immobilized GR. Thereafter, the biosensor probe was dipped in the test solution containing 0.5 mM GSSG. A very clear reduction peak was observed at −0.60 V due to the catalytic reduction of GSSG by NADPH and GR, which clearly demonstrated that the modified electrode responded well to GSSG. In order to completely reduce the test compound, we selected a potential −0.10 V more negative than the reduction potential. Thus, an applied potential of −0.70 V was used to obtain the chronoamperometric response. To obtain a calibration plot, the biosensor was dipped in a blank buffer solution and different concentrations of GSSG were added into the test solution and chronoamperograms were obtained, as shown in Fig. 4(B). A calibration plot (Fig. 4(B), inset (a)) was obtained for concentrations of GSSG between 0.1 μM and 4.0 mM with the dynamic range occurring between 0.1 μM and 2.5 mM. The linear regression equation is expressed as follows: I_p (μA) = 0.66 (±0.49) + 34.38 (±0.59) [GSSG mM], with a correlation coefficient of 0.999. The detection limit for GSSG was determined to be 12.5 ± 0.5 nM (RSD < 5%) based on measurements performed five times for the standard deviation of the blank solution (95% confidence level, $k = 3, n = 5$). This detection limit is lower than the value previously obtained for GSSG using another electrochemical method [12]. The inset (b) in Fig. 4B shows the response current at a steady state after the addition of GSSG, where 95% of steady state currents were achieved after about 10 s. The fabricated biosensor responded within 10 s to GSSG which is acceptable for its in vivo diagnostic applications [27].

We also examined the interference of the electroactive compounds commonly present in real samples. For this purpose, ascorbic acid, uric acid, acetaminophen, and dopamine were examined under the optimized experimental conditions (data not shown). No foreign peaks were observed, which means that these chemical species were not catalytically reduced by the GR-NADPH probe and thus did not interfere with the biosensor. Furthermore, the biosensor was tested in a real plasma sample and no foreign peaks were observed, indicating that none of the plasma components interfered in the detection of GSSG.

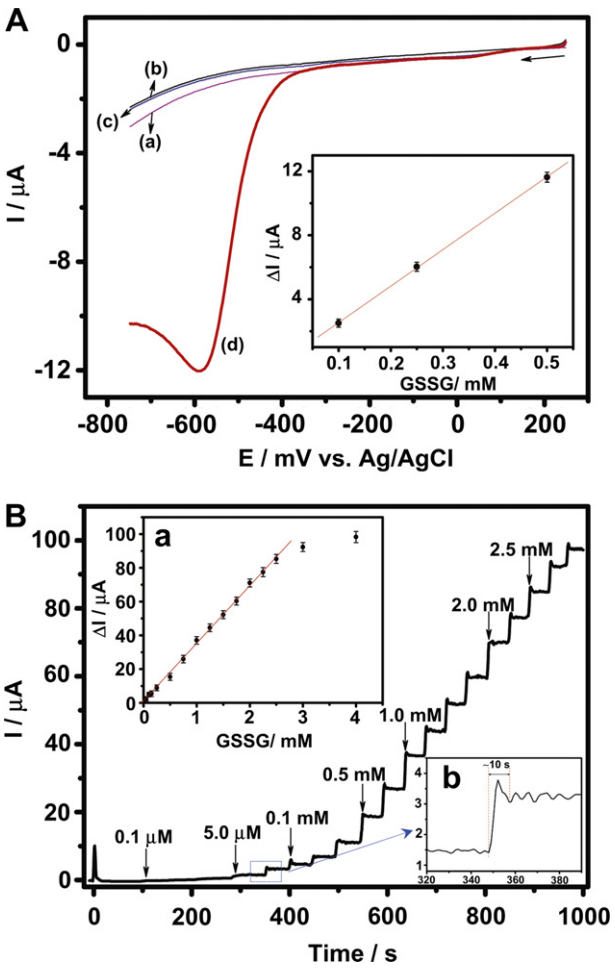

Fig. 4. (A) LSVs recorded for the (a) GR-NADPH/polyTTBA/AuNPs/GCE (magenta line) in 0.1 M PBS (pH 7.4) and (b) NADPH/polyTTBA/AuNPs/GC (black line), (c) GR/polyTTBA/AuNPs/GC (blue line), and (d) GR-NADPH/polyTTBA/AuNPs/GC (red line) electrodes in PBS containing 0.5 mM GSSG. Inset: calibration plot for different concentrations (0.1, 0.25, and 0.5 mM) of GSSG. (B) Chronoamperometric responses observed at the GR-NADPH/polyTTBA/AuNPs/GCE in 0.1 M PBS (pH 7.4) after successive injection of GSSG. Inset: (a) corresponding calibration plot and (b) response time of biosensor. (For interpretation of the references to colour in this figure legend, the reader is referred to the web version of this article.)

The lifetime of the biosensor was determined by monitoring its response with respect to the time of storage. The biosensor was stored in PBS with a pH of 7.4 at 4.0 °C. The response of the electrode was regularly checked every five days and plotted against the storage time (data no shown). The sensitivity of the biosensor for the reduction of GSSG was about 95% of its initial value after a storage time of 10 weeks and then gradually started to decrease. The deterioration of the biosensor response after this time was possibly caused by the denaturation of the immobilized enzyme. These results suggest that the lifetime of the fabricated biosensor electrode is 10 weeks.

3.5. In vivo GSSG analysis

The practical applicability of the biosensor was first investigated through the detection of GSSG in a human plasma sample because

the plasma GSSG concentration is a sensitive index of oxidative stress in the human body [28]. For this purpose, the biosensor was used to detect the GSSG concentration in 25-fold diluted plasma sample. Under the optimized conditions GSSG was detected in the similar dynamic range as in the blank buffer. The obtained calibration plot is shown in (Fig. 5(A), inset chronoamperogram). The linear regression equation for GSSG detection in plasma is expressed as follows: I_p (μA) = 0.52 (±0.38) + 33.64 (±0.70) [GSSG mM], with a correlation coefficient of 0.999. The detection limit of GSSG in plasma samples is 15.6 ± 0.7 nM (RSD < 5%) based on measurements performed five times for the standard deviation of the blank solution (95% confidence level, $k = 3$, $n = 5$). The recoveries of GSSG from the spiked plasma samples were calculated based on the calibration curve and presented in Table 1. The concentration recovery for GSSG was between 94 and 97% with RSD < 5%. These results clearly indicate that the developed biosensor is stable in plasma sample and can detect GSSG in the complex plasma matrix.

The performance of the GSSG biosensor was then examined in vivo, where a microbiosensor was fabricated by a similar approach to that previously reported [13]. The purpose of using a microbiosensor was to monitor the oxidative stress in terms of in vivo GSSG concentrations. First, the microbiosensor was tested for its ability to detect standard GSSG concentrations (Fig. 5(B)). For this purpose, varying concentrations of GSSG were tested using chronoamperometry with a −0.70 V applied potential. The current response increased exponentially for concentrations of GSSG between 0.1 μM and 50.0 μM. The linear regression equation for GSSG detection is expressed as follows: I_p (μA) = 0.07 (±0.029) + 0.025 (±0.001) [GSSG μM], with a correlation coefficient of 0.999. Thus, the fabricated microbiosensor is capable of GSSG detection. The hepatic GSSG formation is a sensitive indicator of oxidative stress [29], which can be induced using diquat and *t*-BHP [21]. Thus, we examined the in vivo GSSG concentrations using a microbiosensor to monitor oxidative stress. First, a transverse abdominal incision was made on with the rats treated with diquat under isoflurane anesthesia. Thereafter, the microbiosensor was inserted into the rats' livers, allowing the experiments to be performed. Fig. 5(C) shows chronoamperograms obtained for (a) blank (no diquat administration) and (b) - (g) after diquat administration. The current response obtained for the in vivo GSSG concentration increases with an increase in the exposure times of diquat from 10 to120 min (RSD < 5%, $n = 5$). For the 10 min exposure time, the current response was low but increased distinctly as the diquat exposure time increased. The increase in the current is due to the formation of more GSSG because of the diquant administration [29].

Table 1
Recoveries of GSSG from spiked plasma sample ($n = 5$).

Sample	Level added (μM)	Level found ± S.D. (μM)	RSD (%)	Recovery (%)
1	0.1	0.095 ± 0.003	3.95	95
2	10.0	9.4 ± 0.38	4.04	94
3	25.0	24.1 ± 0.96	3.98	96
4	50.0	48.6 ± 1.89	3.88	97
5	100.0	96.0 ± 3.94	4.10	96
6	500.0	475.8 ± 18.51	3.89	95
7	1000.0	970.2 ± 38.91	4.01	97

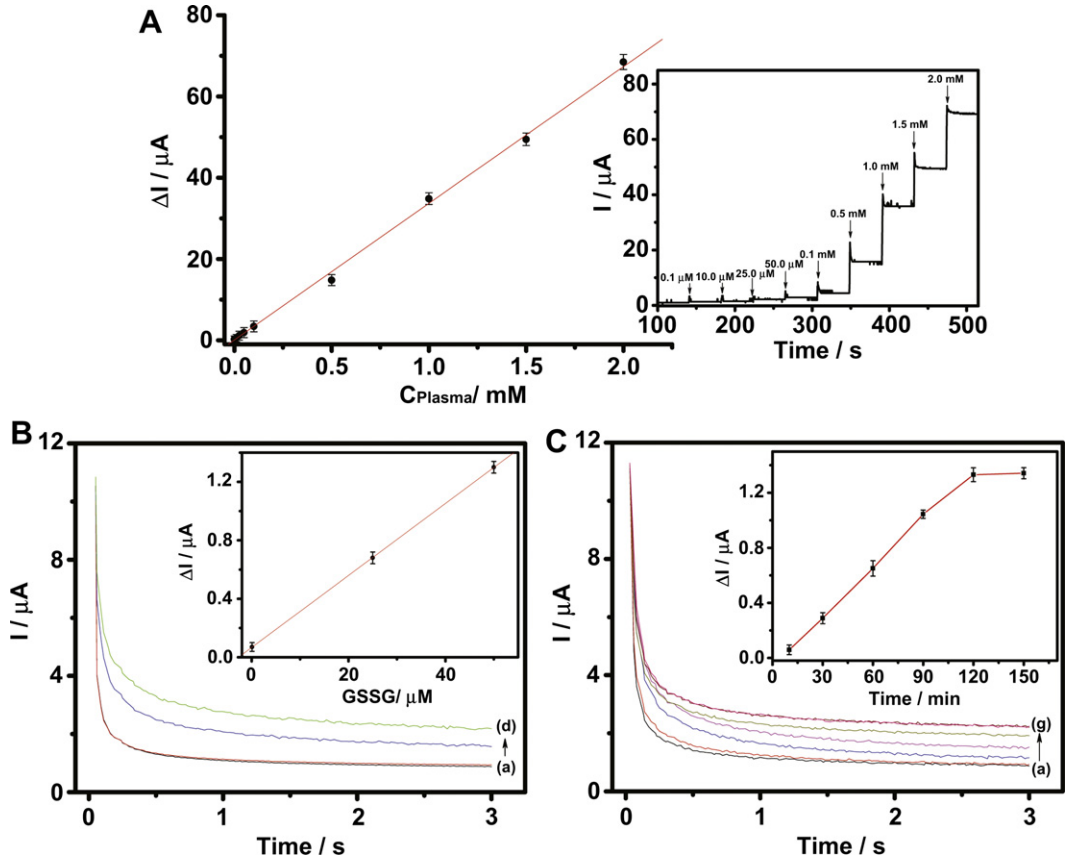

Fig. 5. (A) Calibration plot for the determination of GSSG in real plasma sample (inset: chronoamperogram). (B) Chronoamperograms recorded using a microbiosensor for various standard solutions of GSSG: (a) blank, (b) 0.1 (red line), (c) 25.0 (blue line), and (d) 50.0 (green line) μM (inset: calibration plot). (C) In vivo chronoamperometric responses of GSSG after: (a) 0, (b) 10, (c) 30, (d) 60, (e) 90, (f) 120, and (g) 150 min diquat administration (inset: calibration plot). (For interpretation of the references to colour in this figure legend, the reader is referred to the web version of this article.)

A calibration plot was obtained between diquat exposure time and the current response due to GSSG reduction. The linear regression equation is expressed as follows: I_p (μA) = 0.87 (±0.025) + 0.012 (±0.0003) [GSSG μM], with a correlation coefficient of 0.997. This proves that the fabricated microbiosensor is capable of monitoring oxidative stress as indicated by increased GSSG concentration. The results obtained in terms of increased GSSG concentration with diquat exposure time are in agreement with previously reported results [21]. A similar response was observed when *t*-BHP was administered (data not shown). All in vivo experiments were performed in three separate biological replicates.

4. Conclusions

We have successfully developed a highly sensitive, selective, and stable biosensor for GSSG detection using GR and NADPH immobilized onto a nanocomposite conducting polymer film. The biosensor surface was successfully characterized using SEM, TEM, UV–Vis, XPS, QCM, and electrochemical techniques. The detection limit of the proposed biosensor was 12.5 ± 0.5 nM ($k = 3$, $n = 5$), which is lower than previously reported results. The present biosensor exhibited long term stability of up to 10 weeks and was successfully used to detect GSSG in plasma samples. A GR-NADPH microbiosensor was also fabricated and successfully applied to detect GSSG concentrations in vivo to monitor oxidative stress. The strategy described here has many attractive features: simplicity, rapidity, low cost, and no requirement for a specific label (i.e., a fluorescent or reactive moiety), all of which indicate that this could be a useful method for medical diagnosis of oxidative stress.

Acknowledgment

This work was supported by NRF grants funded by the MEST, South Korea (Grant No. 20100029128).

References

[1] Meister A, Anderson ME. Glutathione. Annu Rev Biochem 1983;52:711–60.
[2] Noctor G, Gomez L, Vanacker H, Foyer CH. Interactions between biosynthesis, compartmentation and transport in the control of glutathione homeostasis and signalling. J Exp Bot 2002;53:1283–304.
[3] Kelly FJ, Mudway I, Blomberg A, Frew A, Sandström T. Altered lung antioxidant status in patients with mild asthma. Lancet 1999;354:482–3.
[4] Aukrust P, Svardal AM, Müller F, Lunden B, Berge RK, Ueland PM, et al. Increased levels of oxidized glutathione in CD4+ lymphocytes associated with disturbed intracellular redox balance in human immunodeficiency virus type 1 infection. Blood 1995;86:258–67.
[5] Annuk M, Zilmer M, Lind L, Linde T, Fellström B. Oxidative stress and endothelial function in chronic renal failure. J Am Soc Nephrol 2001;12:2747–52.
[6] Rahman I, Kode A, Biswas SK. Assay for quantitative determination of glutathione and glutathione disulfide levels using enzymatic recycling method. Nat Protoc 2007;1:3159–65.
[7] Wang H, Liang SC, Zhang ZM, Zhang HS. 3-Iodoacetylaminobenzanthrone as a fluorescent derivatizing reagent for thiols in high-performance liquid chromatography. Anal Chim Acta 2004;512:281–6.
[8] Ates B, Ercal BC, Manda K, Abraham L, Ercal N. Determination of glutathione disulfide levels in biological samples using thiol-disulfide exchanging agent, dithiothreitol. Biomed Chromatogr 2009;23:119–23.
[9] Remião F, Carmo H, Carvalho F, Bastos ML. Simultaneous determination of reduced and oxidized glutathione in freshly isolated rat hepatocytes and cardiomyocytes by HPLC with electrochemical detection. Biomed Chromatogr 2000;14:468–73.
[10] Zhang W, Wan F, Zhu W, Xu H, Ye X, Cheng R, et al. Determination of glutathione and glutathione disulfide in hepatocytes by liquid chromatography with an electrode modified with functionalized carbon nanotubes. J Chromatogr B Analyt Technol Biomed Life Sci 2005;818:227–32.
[11] Banica FG, Fogg AG, Moreira JC. Catalytic cathodic stripping voltammetry of oxidized glutathione at a hanging mercury drop electrode in the presence of nickel ion. Talanta 1995;42:227–34.
[12] Safavi A, Maleki N, Farjami E, Mahyari FA. Simultaneous electrochemical determination of glutathione and glutathione disulfide at a nanoscale copper hydroxide composite carbon ionic liquid electrode. Anal Chem 2009;81:7538–43.
[13] Rahman MA, Kwon NH, Won MS, Choe ES, Shim YB. Functionalized conducting polymer as an enzyme-immobilizing substrate: an amperometric glutamate microbiosensor for in vivo measurements. Anal Chem 2005;77:4854–60.
[14] Morrison DWG, Dokmeci MR, Demirci U, Khademhosseini A. Clinical applications of micro- and nanoscale biosensors. In: Gonsalves KE, Laurencin CL, Halberstadt CR, Nair LS, editors. Biomedical nanostructures. John Wiley & Sons, Inc; 2008. p. 433–54.
[15] Bhattacharyay D, Dutta K, Banerjee S, Turner APF, Sarkara P. Disposable amperometric sensors for thiols with special reference to glutathione. Electroanalysis 2008;20:1947–52.
[16] Lee TY, Shim YB. Direct DNA hybridization detection based on the oligonucleotide-functionalized conductive polymer. Anal Chem 2001;73:5629–32.
[17] Koh WC, Son JI, Choe ES, Shim Y- B. Electrochemical detection of peroxynitrite using a biosensor based on a conducting polymer-manganese ion complex. Anal Chem 2010;82:10075–82.
[18] Lee KS, Won MS, Noh HB, Shim YB. Triggering the redox reaction of cytochrome c on a biomimetic layer and elimination of interferences for NADH detection. Biomaterials 2010;31:7827–35.
[19] Koh WC, Chandra P, Kim DM, Shim YB. Electropolymerized self-assembled layer on gold nanoparticles: detection of inducible nitric oxide synthase in neuronal cell culture. Anal Chem 2011;83:6177–83.
[20] Shiddiky MJ, Shim YB. Trace analysis of DNA: preconcentration, separation, and electrochemical detection in microchip electrophoresis using Au nanoparticles. Anal Chem 2007;79:3724–33.
[21] Madhu C, Gregus Z, Klaassen CD. Marked interanimal differences in susceptibility of Sprague-Dawley rats to diquat-induced oxidative stress in the liver: correlation with hepatic uptake of diquat. J Pharmacol Exp Ther 1992;263:1003–8.
[22] Shim YB, Park SM. Electrochemistry of conductive polymers. 22. Electrochemical and spectroelectrochemical studies of polyazulene growth and its characterization. J Electrochem Soc 1997;144:3027–33.
[23] Chandra P, Noh HB, Won MS, Shim YB. Detection of daunomycin using phosphatidylserine and aptamer co-immobilized on Au nanoparticles deposited conducting polymer. Biosens Bioelectron 2011;26:4442–9.
[24] Chen J, Cai CX. Direct electrochemical oxidation of NADPH at a low potential on the carbon nanotube modified glassy carbon electrode. Chin J Chem 2004;22:167–71.
[25] Li Y, Yang SY, Chen SM. Biosensing approach for glutathione detection using glutathione reductase (GR) with multi-walled carbon nanotubes on gold electrode. Int J Electrochem Sci 2011;6:3982–96.
[26] Mize CE, Langdon RG. Hepatic glutathione reductase. I. Purification and general kinetic properties. J Biol Chem 1962;237:1589–95.
[27] Tian F, Gourine AV, Huckstepp RT, Dale N. A microelectrode biosensor for real time monitoring of L-glutamate release. Anal Chim Acta 2009;645:86–91.
[28] Adams Jr JD, Lauterburg BH, Mitchell JR. Plasma glutathione and glutathione disulfide in the rat: regulation and response to oxidative stress. J Pharmacol Exp Ther 1983;227:749–54.
[29] Jaeschke H. Glutathione disulfide as index of oxidant stress in rat liver during hypoxia. Am J Physiol 1990;258:G499–505.